



# Performance comparison of heat recovery systems to reduce viral contagion in indoor environments

Luigi Schibuola, Chiara Tambani<sup>\*</sup>

University IUAV of Venice, Dorsoduro 2206, 30123 Venice, Italy

## ARTICLE INFO

### Keywords:

COVID-19 airborne diffusion  
Viral contagion  
Ventilation increment  
Indoor environment  
High efficient recovery  
Heat pump

## ABSTRACT

Strong ventilation increments are currently suggested for containing the airborne diffusion of COVID-19 in indoor environments. However, it can involve an unacceptable growing of energy consumption. Therefore, maximum care must be addressed to improve efficiency of ventilation heat recovery (VHR). For this purpose, this paper investigates the opportunity of a technical solution. Consisting in adding downstream of the most diffuse heat recuperator, a heat pump using exhaust air as a cold source. An autonomous high efficiency air handling unit (HEAHU) was modelled for a school application. By simulation a performance comparison was carried on with two alternative systems based only on an exhaust air heat pump (EAHP) or on a heat recuperator for different weather conditions. Results indicated that the milder climate strongly penalizes heat recuperator and this fact deeply influences the conclusions. HEAHU saving compared to energy consumption of only heat recuperator is between 31% and 46%. For EAHP this saving varies from 2.5% to 48%. Only with a milder climate, EAHP presents a lightly greater saving than HEAHU. Heat pump technology looks to be very performing to foster the efficiency of VHR, especially in presence of high ventilation rates.

## 1. Introduction

On the basis of current scientific evidence, as for other viral diseases international health authorities indicate multiple transmission routes for COVID-19 and mostly airborne transmission by droplets, direct contact with an infected person or contact with a surface previously contaminated by infected people or by deposition of viral particles [1].

Indoor airborne transmission between occupants takes place mainly from the emission of infectious droplets from an infected person, their spread in the indoor environment and their inhalation by susceptible individuals [2–4]. Current studies show that droplets from human respiration activities are mostly less than 10  $\mu\text{m}$  in diameter [5–11]. The majority of these droplets evaporates and it is quickly reduced to half of their initial size [3]. Consequently, they are called droplet nuclei or aerosols when their diameter is less than 5  $\mu\text{m}$  [12].

In indoor environments virus-laden aerosols may easily accumulate and consequently airborne diffusion mechanism of COVID-19 is a topic of high interest [13,14]. In addition, many viruses are characterized by a long lifetime in aerosols [15–17] and by the capacity to penetrate into the lower respiratory system [15,18–20]. Evidence is growing that in addition to contact and droplet spread, the virus transmission via

aerosols is an important contagion mechanism in indoor environments with poor ventilation and long exposure time to high viral concentrations [21]. Many outbreaks in crowded indoor environments such as offices, restaurants, schools, religious gatherings, commercial facilities, cruise ships indicate that airborne virus transmission is particularly efficient in these types of confined space [22]. On the other hand, for long ago research findings have highlighted that poor ventilation contributes to the spread of other similar airborne diseases [23–26]. Airborne transmission can be reduced by indoor air change increment [23,27]. In fact the outdoor air introduction in indoor environments by natural or mechanical way gives an important contribution in removing exhaled virus-laden air, thus lowering the viral concentration and in this way the subsequent dose inhaled by susceptible occupants [14]. Therefore, the recently updated guidelines recommend a significant increase in the amount of fresh air supplied to spaces [28,29]. To quantify the effect of air changes per hour (ACH) on contagion risk in indoor environment, the well-recognized Wells-Riley model can be used [30,31]. The outcomes indicate a close correlation between ventilation increase and contagion risk decrease [32] with a fall in value of the infection probability with ACH above 10  $\text{h}^{-1}$  [33]. However, many scientific uncertainties are still present about contagion dynamics. For this reason specific standards about precise ACH values required in

<sup>\*</sup> Corresponding author.

E-mail address: [chiara.tambani@iuav.it](mailto:chiara.tambani@iuav.it) (C. Tambani).

## Nomenclature

### Symbols

ACH	Air changes per hour ( $\text{h}^{-1}$ )
AHU	air handling unit
CF	capacity factor $P_{fl}/P_{nom}$ (-)
CR	capacity ratio (-)
COP	coefficient of performance (-)
$D_p$	air pressure loss (Pa)
$E_p$	primary energy (kWh)
EAHP	exhaust air heat pump
HEAHU	high efficiency air handling unit
HVAC	heating ventilation and air conditioning
$h$	specific enthalpy (kJ/kg)
IAQ	indoor air quality
$\dot{m}$	air mass flow rate (kg/s)
$P$	actual capacity of the heat pump (kW)
$P_{fl}$	full load heat pump capacity (kW)
$P_{nom}$	nominal heat pump capacity (kW)
PER	primary energy ratio (-)

PLF	part load factor (-)
$P_{fan}$	fan electric absorption (kW)
$P_{boiler}$	thermal power from boiler (kW)
$P_{rec}$	recovered thermal power (kW)
OHR	only heat recuperator
RH	relative humidity (%)
$t$	air temperature ( $^{\circ}\text{C}$ )
$\dot{V}$	air volumetric flow rate ( $\text{m}^3/\text{s}$ )
VHR	ventilation heat recovery
$X$	absolute humidity (g/kg)
$\eta_t$	thermal efficiency of the recuperator (-)
$\eta_f$	fan efficiency (-)

### Subscripts

$i$	indoor
$o$	outdoor
exro	expulsion air at recuperator outlet
fl	full load
net	without fan
el	Electric

pandemic conditions have not been introduced yet. Meanwhile, new researches must be performed to solve the technical, energy and economic problems related to a remarkable ACH increase in order to improve its feasibility both in existing and new ventilation systems.

In the school environment, the exigency of adequate ventilation is of great concern already under no pandemic conditions. In fact, school environments are characterized by elevate occupancy density in comparison with residential buildings and many offices or commercial facilities. Despite that students spend a significant time in classrooms, the ventilation rate is often insufficient [34–36]. In particular in naturally ventilated classrooms an adequate ventilation air flow rate is difficult to achieve, because it depends on specific local conditions like sizes and position of openings, weather conditions and airing management. In fact often human behavior dictated by indoor comfort or safety requirements may cause openings remain closed, in particular when outdoor weather is too hot or cold. For this reason mechanical ventilation systems are recommended for classrooms and this necessity is going to be strengthened by the exigency to contrast current and future outbreaks.

An important question concerns the modification of the existing mechanical ventilation systems which were being designed for no pandemic condition. The requirement of the large amount of outdoor air to be supplied during outbreaks can be difficult to meet without significant transformations. In fact mechanical ventilation is often implemented in the heating, ventilation and air conditioning (HVAC) systems which also provide heating and air conditioning in the buildings. New additional design criteria are needed by HVAC engineers to contrast virus airborne diffusion. For this reason, international HVAC guidelines have quickly been updated to address this new exigency [37,38]. Future HVAC systems will have to be designed to supply large ventilation rates during pandemic periods, but they will be able to operate economically with strongly reduced outdoor air flows under no pandemic conditions thanks to the implementation of demand controlled ventilation (DCV). This control technique fits the actual flow rate needs in order to use the minimum amount of energy necessary to grant comfort and, especially in this case, health conditions. Its application in presence of large flow rate modifications causing by high occupancy variability, has already widely demonstrated the ability to provide strong energy savings [39–42]. Therefore, it can be profitably used also to manage HVAC systems in the change from pandemic to no pandemic condition.

However, a strong increase in ventilation rates can also involve an unacceptable increment of energy consumption and consequently of energy cost and  $\text{CO}_2$  gas emission in atmosphere. Therefore, great effort

must be dedicated to increase energy efficiency of ventilation heat recovery (VHR).

This study deals with the improvement of energy recovery in ventilation to be achieved by systems expressly designed to operate also in pandemic condition and evaluated for specific contexts. In this analysis, the context concerns with the school environment, which is a strategic context, especially in this pandemic condition, with the proposal of an autonomous air handling unit (AHU) to be installed in a single classroom. This solution can be applied also in retrofit actions to reduce viral risk in the existing naturally ventilated classrooms which are the majority in Southern Europe.

In this analysis, a maximization of the heat recovery from exhaust air is pursued by the introduction of a heat pump downstream of the heat recuperator in order to obtain a further recovery from exhaust air by its use as cold source of the heat pump. Heat pump using outside air as cold source can be heavy penalized in some winter periods as a low air temperature at the evaporator reduces its efficiency. Instead, the defects of the outside air are not attributable to exhaust air which presents a more favorable and less variable thermal level. This fact indicates the opportunity to consider its use as cold source for the heat pump in VHR systems. The coupling of an exhaust air heat pump with a heat recuperator is a technical solution indeed rarely used except in some cases like indoor swimming pools [43,44]. In this case, owing to the low absolute humidity of outdoor air in winter, high outdoor air flow rates are used to control indoor relative humidity in presence of the evaporation of the pool. Consequently, the exhaust air flow rate is at the top. In all the other HVAC system, the heat recuperator is normally more widespread, because simpler and cheaper. But now the risk of a drastic increment of the energy consumption in the case of the adoption of the new ventilation requirements, imposes the need to study a generalized improvement of VHR system efficiency. This necessity suggests investigating the use of the considered solution also in other applications. In fact, thanks to a greater energy efficiency of the recovery from the exhaust air, HEAHU can be able to provide a remarkable increase of saved energy amount as consequence of the strong air flow rates. However, this conclusion is not obvious. The effective energy superiority must be verified depending on the application context and the climate [45,46]. This is the object of this study which compares three different VHR systems in a school environment and for different climates.

Virus transmission via heat recovery devices is not an issue when there is a net physical air separation between the return and supply side. Among the various recovery systems of this kind, counter-flow

recuperator was considered here as representative. Instead, rotary heat exchangers can have significant leakage from the exhaust air side to the supply air side in case of poor design, bad installation or maintenance [47]. Therefore, in the event of installation of heat exchanger wheels, frequent periodic inspections are absolutely necessary to avoid the risk of internal leakages [37]. Also for this reason they were not considered here, even if rotary wheels with desiccant material coating permit a moisture recirculation able to reduce latent load.

The proposed technical solution was applied to an autonomous high efficiency air handling unit (HEAHU) for the installation in existing naturally ventilated or new classrooms when centralized ventilation recovery systems are not possible or convenient. A simulation model was elaborated to assess the energy performance of HEAHU and to compare its convenience with a recovery system with only an exhaust air heat pump (EAHP) [48–50] or with only heat recuperator (OHR). These evaluations were carried on by considering the case study of a typical high school classroom in Italy. To investigate the influence of the climate, the simulations were extended to winter season for three cities: Milan, Rome and Palermo, well distributed in Italy and therefore considered representative of weather conditions in Southern Europe. The study analyses a wide range of specific ventilation air flow rate per person: from a minimum value to ensure acceptable indoor air quality (IAQ) in the classroom up to four times this value. In the current absence of precise ACH values required to control indoor airborne contagion, the goal is to validate the results for a large spectrum of possible ACH requirements that could be indicated by health authorities on the basis of actual and future scientific findings. In synthesis the objectives of this work consist in: i) the development of an autonomous unit suitable to operate in a school environment even in pandemic conditions, ii) the elaboration of a specific model able to permit the hourly simulation of the unit extended to the heating season, iii) the energy performance comparison of three possible technical alternatives in different climatic conditions.

## 2. Materials and methods

### 2.1. Case study

The study analyzes the possibility to install a mechanical ventilation system in an existing classroom naturally ventilated in origin, which is a very widespread reality in Southern Europe. A typical classroom of a high school was considered with a standard occupancy of 25 students plus the teacher. Its dimensions are reported in table 1. Lesson schedule is typical for high schools in Italy. Classrooms are open from Monday to Friday and used from 8AM to 1.30PM. Mechanical ventilation only works in these time intervals. Holiday periods were considered. As regards the ventilation flow rate, current standards consider different ventilation categories on the basis of different amounts of supply air per person, [51,52]. Standards also recommend additional clean air to remove pollution emitted by building materials. In detail the supply ventilation rate is the sum of the air volume required for each occupant defined in four categories (Cat I – 10 l/s/pers, Cat II – 7 l/s/pers, Cat III – 4 l/s/pers, Cat IV – 2.5 l/s/pers) plus additional air flow rate (l/s/m<sup>2</sup>

**Table 1**  
Characteristics of the classroom and climatic data of the three localities.

Classroom	Location	Milan	Rome	Palermo
Surface (m <sup>2</sup> )	51	Latitude 45.5°	41.9°	38.1°
Height (m)	3.2	Degree days 2404	1415	751
Volume (m <sup>3</sup> )	163.2	Design temperature -5°C	0 °C	+5°C
Students + teacher	26	Heating start 15th October	1st November	1st December
Density (pers/m <sup>2</sup> )	0.51	Heating end 15th April	15th April	31st March

of floor area) for building materials pollution removal obtained considering three different possible emission levels of the building. For the intermediate level (low polluting buildings) this additional air flow rate assumes one of the values: 1.0, 0.7, 0.4, 0.3 l/s m<sup>2</sup> going from Cat. I to Cat. IV, respectively.

However, to generalize the outcomes, in this study the new ventilation rates are based only on the occupancy with a minimum value of 8 l/s/pers (29 m<sup>3</sup>/h) able to ensure a medium IAQ as indicated by the previous standards. In presence of viral emergency, it was assumed that this value would grow up to four times (32 l/s/pers). But to investigate the behavior of VHR systems along this wide range, two intermediate air flow rates (16 and 24 l/s/pers) were also considered in the simulation. For the analysed case study, it means an air flow rate range between 749 and 2995 m<sup>3</sup>/h and ACH between 4.6 and 18.3 h<sup>-1</sup>. In Italy school period is from September to June and only heating systems are normally foreseen in high schools. Therefore, the investigations were limited to the heating season. Data about the heating season of each considered location are in table 1. Performance simulations extended to the heating season were carried on by utilizing weather files from [53]. The sizing of the components of the investigated systems was obtained on the basis of the design temperatures. In particular the required capacity of each heat pump eventually present was calculated for each ventilation rate at the design climatic condition reported in table 1 for each city. On the basis of the performance data from the manufacturer, as usual, this capacity allows the designer to individuate the size and consequently the nominal capacity of the heat pump. For an air source heat pump this nominal capacity normally refers to an outdoor temperature of 7 °C and relative humidity (RH) 90%.

Indoor design condition is 20 °C and RH equal to 50%. As we assume a heating system (usually radiators) already existing in the classroom, a neutral temperature of 20 °C is foreseen for the fresh air supply. In this case RH equal to 50% corresponds to an absolute humidity of 7.4 g/kg. But owing to the presence of 26 persons in the classroom, there is an indoor latent gain here considered of 60 W/person (sedentary activity) which corresponds to an indoor emission of 2.25 kg/h of vapor. Therefore, the air introduced can present a lower absolute humidity to maintain RH at 50%. With 8 l/s/pers the reduction is about 2.5 g/kg and therefore immission air absolute humidity is equal to 4.9 g/kg. This fact has an influence on the calculation of the latent quota of the ventilation load consequent the necessary humidification treatment of the intake air during the heating season. Of course a doubling of the ventilation flow rate (16 l/s/pers) corresponds to a halving of the absolute humidity reduction and so on with the increasing of ventilation rate.

### 2.2. The three recovery systems

In modern HVAC systems, centralized mechanical ventilation units normally include heat recovery from exhaust air. The intervention on new or existing centralized AHUs in order to increase ventilation rate can be accompanied by a fostering of the heat recovery by the addition of an air-to-water heat pump downstream the recuperator. This solution presents high flexibility. Hot water from condenser can be used to meet different demands, from space heating to domestic hot water production. But the solution of new centralized ventilation systems is often unfeasible for technical or economic obstacles. Also the energy consumption analysis can indicate a different solution.

In fact, ventilation heat recovery systems may be centralized, semi-centralized or decentralized. This choice influences the energy performance [54] and sometimes decentralized AHUs can give the best energy performance. In [55] savings in fan energy consumption of 40 and 80% were calculated for the semi-centralized and decentralized units, respectively, if compared to the centralized ones. Furthermore, disadvantages about the centralized system might be fostered by the growing air flow rate in pandemic conditions owing to higher initial costs associated with more voluminous ducting systems as well as greater fan management cost. In this paper the alternative of an autonomous AHU

for each classroom was considered. Fig. 1a shows the scheme of the proposed HEAHU where an air-to-air heat pump is coupled with a cross flow countercurrent air-to-air heat exchanger. Similar units are already present on the market [56], but in this case, the further adding of a humidifier must be foreseen, certainly necessary in the heating period owing to the strong increase of the outside air flow rate. In fact scientific literature indicates as low RH facilitates infection diffusion [57]. In particular RH below 40% impairs mucus membrane barriers and other levels of the immune system protection [58]. In addition, many viruses are anhydrous resistant and have increased vitality in low RH conditions [59]. In the analyzed climates, the preheating of the inlet air by the recuperator normally permits an adequate humidification with a typical

saturation efficiency of the humidifier equal to 80%. For the installation in colder weather conditions, to achieve the required RH can be necessary to foster humidification in the unit or directly in the classroom. Another solution is to split the condenser in two units and to insert the humidification device between them to increase preheating before the humidification in order to always achieve the indoor design RH equal to 50%. This option is not considered in this HEAHU. Instead, this solution was adopted in the second recovery system (Fig. 1b) which consists only in an air-to-air heat pump using in this case directly return air as a cold source (EAHP). The third recovery system (Fig. 1c) presents only the heat recuperator with the same characteristics of that one of HEAHU (OHR system). In this case a post heating coil supplied by hot water

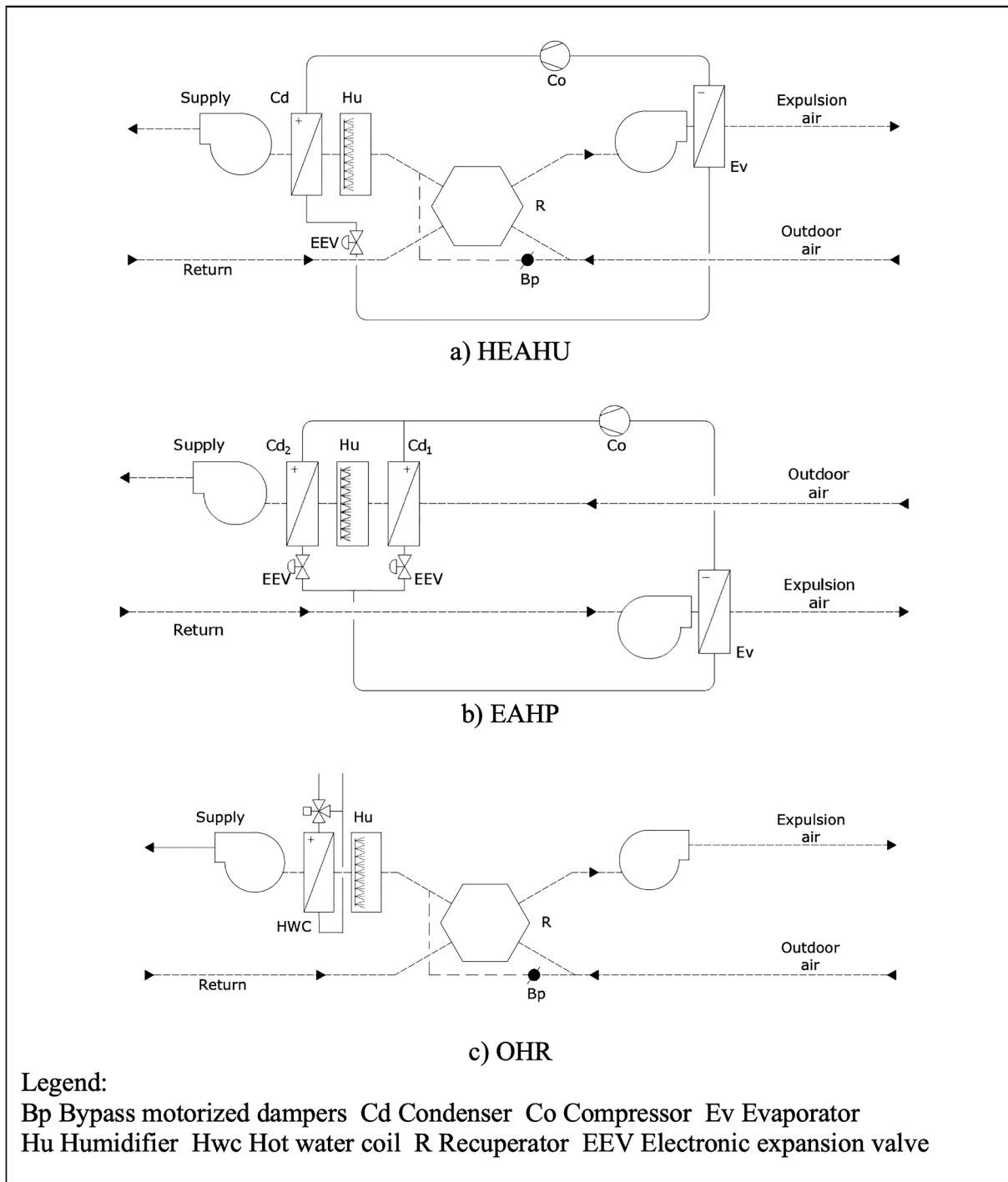


Fig.1. Schemes of the three recovery systems analyzed in the paper.

produced by a boiler is foreseen downstream of the humidifier. In presence of a heat recuperator a bypass controlled by a motorized damper is installed for two reasons. The first reason it is the possibility that the outside air bypasses the heat recuperator when convenient (free heating). The second reason is the possibility to modulate the actual outdoor air flow rate at the inlet of the recuperator by diverting part of it through the bypass damper. In this way, the recovery effect is reduced and the temperature of the exhaust air at the outlet of the recuperator is higher. When the outside temperature is colder, it is so possible to avoid ice formation on the recuperator and the following evaporator. The diverting flow control is based on a minimum value of exhaust air temperature at the recuperator outlet where a temperature sensor is foreseen. This set point is fixed at +3 °C for HEAHU to have no ice in the recuperator and negligible defrosting requirement for the heat pump. For the OHR system a set point temperature of +1 °C is sufficient to avoid ice in the recuperator. Of course for EAHP there is no defrosting problem at the evaporator. Especially in colder climates frost formation is a critical factor which can affect the performance of ventilation units with counter-flow heat exchangers [60,61]. Therefore, the risk of frosting at harsher weather conditions must always be avoided and there are various techniques to address the issue of frost formation [61–63]. In order to prevent air infiltration from the outside, in VHR systems supply and exhaust air flow rates are normally somewhat unbalanced. But in this study, assuming a possible epidemic event, they are considered equal because even a modest superiority of supply air flow rate could cause a transfer of infected air from the classroom to the access corridor and other rooms.

Some fundamental characteristics of the three systems assumed in this analysis are reported in table 2. They are derived from typical values normally used in the design of commercial AHUs [64–66]. In particular to obtain a generalizable

comparison, pressure increase to win pressure losses outside the devices was not considered here, because it can be very variable for the same system on the basis of the installation site characteristics and independent of the internal performances of the unit. In the case of HEAHU, the internal pressure loss  $D_p$  considered in the calculations (eq.14) takes into account the air pressure losses in the heat recuperator on the two sides and in the two coils (condenser and evaporator). For EAHP  $D_p$  considers only three coils (two condensers and evaporator). Heat recuperator and hot water coil for the OHR system. Recuperator thermal efficiency (eq.5) is defined according to EN 308 [67]. Fan efficiency  $h$  includes motor plus belt performance.

### 2.3. HEAHU modeling

For the HEAHU modeling, a quasi-steady state calculation procedure based on a spreadsheet style model was used which operates on each hourly time step. At each time-step, this simulation procedure permits to assess the hourly mean values of the desired quantities on the basis of the mean averages of the input values required by the algorithms which describes the phenomenon studied. This approach is widely used by many well-known dynamic simulation codes as for example TRNSYS [68] and EnergyPlus [69] to evaluate the performance of HVAC systems and components in the long term (seasonal, annual) hourly simulation of the building-plant system. The flow chart of HEAHU model is shown in Fig. 2. The starting point is the calculation of the total ventilation load  $P_{load}$  required to take the supply air from the actual outdoor thermodynamic condition to the input level necessary to ensure design

**Table 2**  
Fundamental characteristics of the three systems.

	HEAHU	EAHP	OHR
Internal pressure loss $D_p$ (Pa)	705	210	665
Recuperator thermal efficiency	0.8	–	0.8
Fan efficiency	0.6		

indoor condition. Since we are in the heating season, if the outside air temperature is greater than the design indoor temperature the system is bypassed by the motorized damper (free heating). In addition, if outdoor absolute humidity is greater than the required absolute humidity of supply air, no humidity treatment is foreseen.

In the other conditions the air handling unit takes the outdoor air to internal design temperature (20 °C) and to the inlet absolute humidity required to ensure an indoor RH equal to 50%. It means that inlet absolute humidity varies on the basis of air flow rate and of internal latent sources due to the attendees. In the end, the  $P_{load}$  can be calculated at every time-step on the basis of the inlet/outlet enthalpy gap of the supply air in the unit and of the supply mass air flow rate  $\dot{m}_{supply}$ :

$$P_{load} = \dot{m}_{supply}(h_{imm} - h_o) \quad (1)$$

The calculation of the energy performance of the HEAHU is obtained in three following steps here reported.

First the evaluation of the heat recovery by the use of recuperator thermal efficiency  $\eta_t$  as defined in EN 308 [67,70] and reported in eq. (2) which permits to calculate the temperature  $t_{exro}$  of the expulsion air at the recuperator outlet on the basis of the indoor air temperature  $t_i$  and outside air temperature  $t_o$

$$\eta_t = \frac{t_{exro} - t_o}{t_i - t_o} \quad (2)$$

$$t_{exro} = t_i - \eta_t(t_i - t_o) \quad (3)$$

If temperature  $t_{exro}$  is higher than the dew point temperature, it means there is no condensation in the exhaust air and its absolute humidity is the same of the return air. Instead, if this outlet temperature is lower than dew point, there is condensation and RH is 100%. In both the cases, psychrometric calculations (eq. (4) to eq. (6)) provide the enthalpies of the exhaust air at the inlet/outlet of the recuperator as functions of temperature and relative or absolute humidity. The fundamental algorithms of psychrometrics are here used [71,72]. Consequently, the total heat recovery  $P_{rec}$  is calculated by this enthalpy gap multiplied by the mass flow rate  $\dot{m}_{ex}$  of the exhaust air (eq. (7)).

$$\text{If } t_{exro} \leq t_{dp} = f(t_i, X_i) \text{ then } h_{exro} = f(t_{exro}, RH = 100\%) \quad (4)$$

$$\text{If } t_{exro} > t_{dp} = f(t_i, X_i) \text{ then } h_{exro} = f(t_{exro}, X_i) \quad (5)$$

$$h_i = f(t_i, RH_i) \quad (6)$$

$$P_{rec} = \dot{m}_{ex}(h_i - h_{exro}) \quad (7)$$

The percentage quota  $\varepsilon$  of the total ventilation load provides by the recuperator can be expressed in terms of eq. (8):

$$\varepsilon = 100 \frac{P_{rec}}{P_{load}} \quad (8)$$

The second step is the calculation of the heat pump circuit performance. The actual heat pump capacity  $P$  must be equal to the load quota not covered by the heat recovery  $P_{rec}$ :

$$P = P_{load} - P_{rec} \quad (9)$$

Before proceeding with the hourly simulation, it is necessary to size the heat pump in each case study i.e. to calculate its nominal capacity. The required design capacity  $P$  is obtained by the previous equations applied in design conditions of outdoor RH (90%) and temperature for each city. Data from manufacturer [64] provides the corresponding nominal rating capacity  $P_{fnom}$  at 7 °C and RH 90%. In this way, full load performance in terms of efficiency and capacity rating can be obtained from Fig. 3a for different air temperatures at the evaporator inlet and for a fixed temperature of 20 °C for the air leaving the condenser. In fact heat pump performances are deeply influenced by the thermal levels at evaporator and condenser. For an air to air heat pump they depend on the air temperature at evaporator inlet and air outlet temperature at the



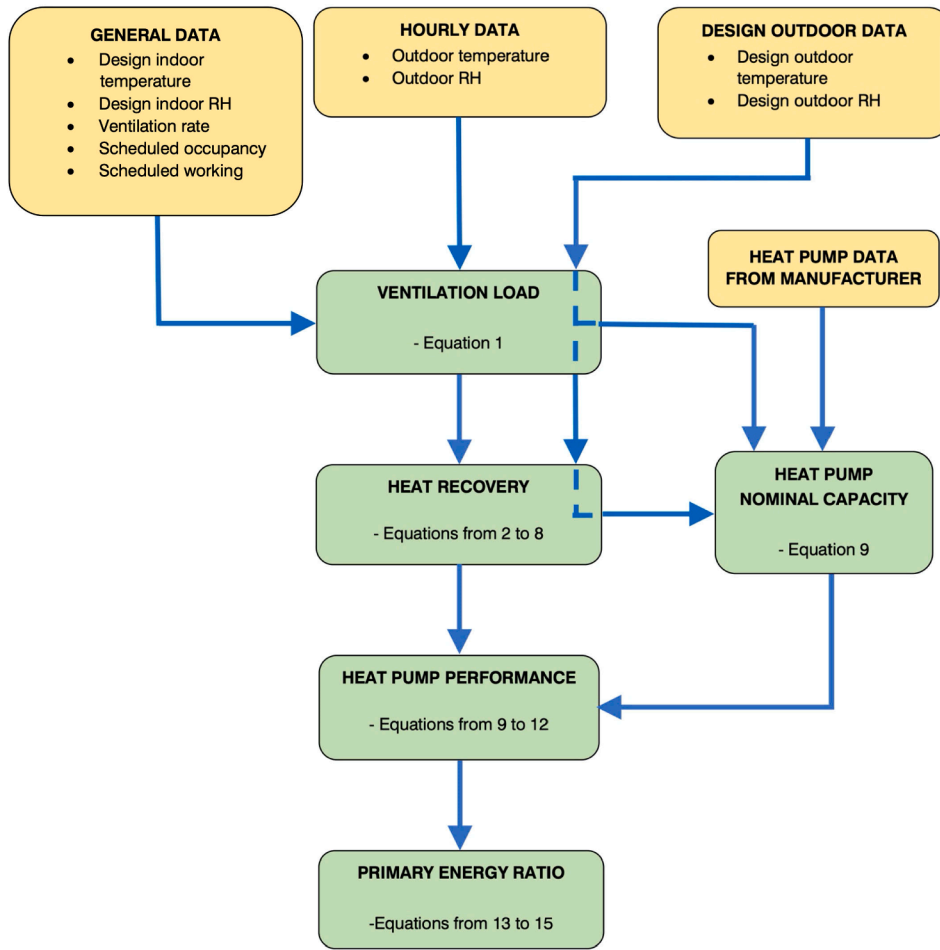


Fig. 2. Flow chart of HEAHU model [67,70].

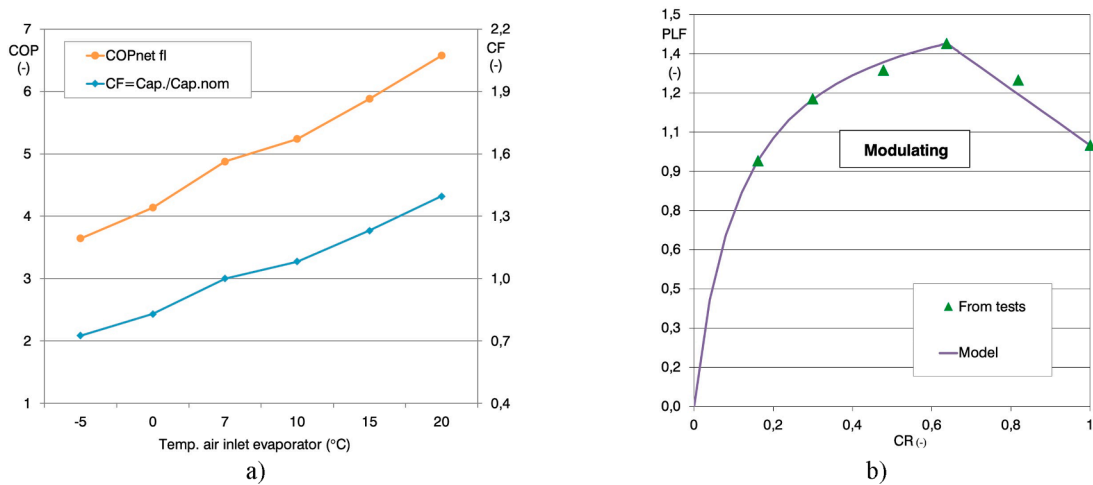


Fig. 3. Capacity factor CF and COP<sub>netfl</sub> as a function of air temperature at evaporator inlet (a) and correction factor PLF as a function of capacity ratio CR (b).

condenser. In this case the air outlet temperature is fixed at 20 °C and therefore in Fig. 3a the performance curves at full capacity are expressed as a function of only air temperature at evaporator inlet. The figure refers to the working fluid R410a. The capacity rating is referred to the nominal rating capacity  $P_{flnom}$  by a capacity factor CF introduced as the ratio between  $P_{fl}$  and  $P_{flnom}$ . It represents the variability of actual full capacity  $P_{fl}$ , referred to the nominal capacity  $P_{flnom}$ , as a function of air temperature at evaporator inlet. CF can be obtained from Fig. 3a. In this

way the model can use data from Fig. 3a for the units with different capacity considered in this study. Consequently the actual full capacity of the heat pump  $P_{fl}$  for different air temperature at evaporator is calculated by CF (eq.10).

$$P_{fl} = P_{flnom} CF \tag{10}$$

Owing to the presence of the recuperator, we have a strong increment of the fan electric absorption of this unit with respect to normal

heat pumps. For this reason, here  $COP_{netfl}$  is the efficiency of the only heat pump circuit without considering fan electric absorption i.e. it is the ratio between heating capacity and only compressor electric absorption. These data come from the manufacturer and they were obtained as required by standard test methods [73]. In the considered heat pump there is only one refrigerant circuit with a single scroll compressor. The actual capacity equal to the load to be met is obtained by a compressor speed modulating control by an inverter device. In order to take into account the effect of part load working condition, a correction factor PLF is introduced for the efficiency at full load capacity  $COP_{netfl}$  [74]. This approach is validated by international regulations [74] and used in research activity about the performance assessment of heat pumps in real working conditions [75–77]. Its trend is reported in Fig. 3b as a function of the capacity ratio CR which is the ratio of the actual capacity on the full capacity that the machine is able to provide at the same level of operating temperatures:

$$CR = P/P_{fl} \quad (11)$$

The PLF curve interpolates data obtained by laboratory tests [78]. PLF is greater than one in a wide range of CR. This result is mainly due to the over-sizing of evaporator and condenser in part load operation rather than in full load.

The actual  $COP_{net}$  is obtained by multiplying the  $COP_{netfl}$  from Fig. 3a by the PLF obtained from Fig. 3b:

$$COP_{net} = COP_{netfl} PLF \quad (12)$$

The electric consumption of the compressor results from the ratio of the output capacity P on the simultaneous  $COP_{net}$ :

$$P_{elnet} = P/COP_{net} \quad (13)$$

In the third step the electric consumption of the fans  $P_{fan}$  is calculated as:

$$P_{fan} = \frac{\dot{V}Dp}{\eta_f 10^3} \quad (14)$$

where rate  $\dot{V}$  is the volumetric flow rate, Dp is the total pressure increase of the fans which is reported in table 2 for each system studied. Fan efficiency  $\eta_f$  is equal to 0.6. The total heating capacity provided by the unit is equal to the load  $P_{load}$  and it is the sum of the recovered heat  $P_{rec}$  and the capacity P of the heat pump. The corresponding total electric absorption is the sum of fan consumption  $P_{fan}$  and compressor input power  $P_{elnet}$ . For a correct comparison with the OHR system, the total energy efficiency was expressed in terms of primary energy ratio PER i.e. the ratio between supplied total heating capacity and the corresponding primary energy consumption. The official Italian value of 2.42 [79] was used to transform the electrical energy need of the device into the corresponding primary energy:

$$PER = \frac{P_{load}}{(P_{fan} + P_{elnet})2.42} \quad (15)$$

The seasonal PER is the ratio of the seasonal heating energy provided and the total primary energy absorption in the same period.

#### 2.4. Modeling of EAHP and the OHR system

In both the cases the models are a simplification of the previous one. In the case of EAHP, the recuperator is not installed and therefore the return air from the classroom is sent directly to the inlet of the evaporator. The whole ventilation load is provided by the heat pump. The total pressure loss is reduced as shown in table 2.

For the OHR system, the total energy consumption consists in the electric absorption of the fan and in the required  $P_{boiler}$  provided by the heating coil supplied with hot water. In this second case the primary energy need is calculated in terms of primary energy  $E_p$  of the natural gas consumed by a typical condensing boiler to produce the heat

necessary for post heating. A seasonal condensing gas boiler efficiency was assumed equal to 0.98 from national standard [80]. Owing to the extreme variability of possible hydraulic circuit options and distances from the boiler, the pumping electric consumption to supply the heating coil was not considered in this analysis. Of course, there is the awareness that its amount can clearly affect the final energy performance of the OHR system. This fact was considered in the discussion of the results. The PER is calculated in this case as:

$$PER = \frac{P_{load}}{\left( P_{fan} 2.42 + \frac{P_{boiler}}{0.98} \right)} \quad (16)$$

The new total internal air pressure loss is reported in table 2.

### 3. Results and discussion

In Fig. 4a monthly and seasonal total ventilation loads are reported for the various cases, while Fig. 4b shows their corresponding percentage latent quotas. It is remarkable the strong difference of the ventilation load in the three cities and its extreme variability at monthly levels which permits to investigate the behavior of the analysed systems in a wide range of conditions. It is evident the influence of indoor latent gains which reduces the necessity of humidification of the input air and so of the latent quota when the ventilation rate is 8 l/s/pers. Growing the ventilation rate, the effect of the indoor latent contribution becomes negligible. In these conditions, the high percentage latent quotas highlight the importance of the humidification requirement. Furthermore, noteworthy is the comparison of these latent quotas in the various cases. At seasonal level, the humidification load quota is greater first in Palermo and then in Milan rather than in Rome. Instead, at monthly level, this comparison provides variable answers. Therefore, stronger latent load quotas are not necessarily related to colder climates.

Fig. 5 shows monthly and seasonal average percentage quotas  $\epsilon$ ,  $COP_{net}$  and PER with HEAHU in the various cases. The variability of the percentage quota  $\epsilon$  highlights the importance of the meteorological conditions on the recuperator performance.

This is evident both at monthly and seasonal level. A greater indoor/outdoor temperature gap increases heat recovery amount by recuperator. Furthermore, colder climate involves more frequent latent heat recovery from the cooling below dew point temperature of the exhaust air in the recuperator. Indoor latent gain reduces the total ventilation load and consequently it clearly improves the percentage quota  $\epsilon$  with 8 l/s/pers intake air flow. But this advantage is decreasing with the growing of the air supply. At seasonal level, in Milan quota  $\epsilon$  varies from 82% to 69%, in Rome from 77% to 65%, from 71% to 53% in Palermo. The  $COP_{net}$  of the refrigerator circuit depends on the inlet evaporator temperature and part load working effect. The first parameter is strictly connected to the recuperator performance, because it coincides with the exhaust air temperature at recuperator outlet. Thanks to the capacity control by inverter, part load increases  $COP_{net}$  in a wide range of the capacity ratio CR, instead it strongly penalizes  $COP_{net}$  in the event of CR below 0.2. The combined effect of these two parameters provides an average  $COP_{net}$  without great oscillations in each locality. PER is strongly influenced by fan electric energy consumption which is constant for each ventilation rate independently by recuperator and heat pump working conditions. Only with the best percentage quotas  $\epsilon$  at monthly level, especially in Milan, a relevant PER increase is evident.

In Fig. 6 monthly and seasonal average  $COP_{net}$  and PERs with EAHP are reported. In this case return air from inside is directly submitted to the evaporator and therefore the air temperature at the evaporator inlet is 20 °C. A so favourable thermal condition causes a strong increment of  $COP_{net}$ , but the performances remain influenced by the different climatic conditions also in this case of EAHP with constant thermohygrometrical characteristics of the exhaust air at evaporator inlet. In fact the actual capacity provided by EAHP is a consequence of the total load and relative percentage latent quota determined by climate. Therefore, the

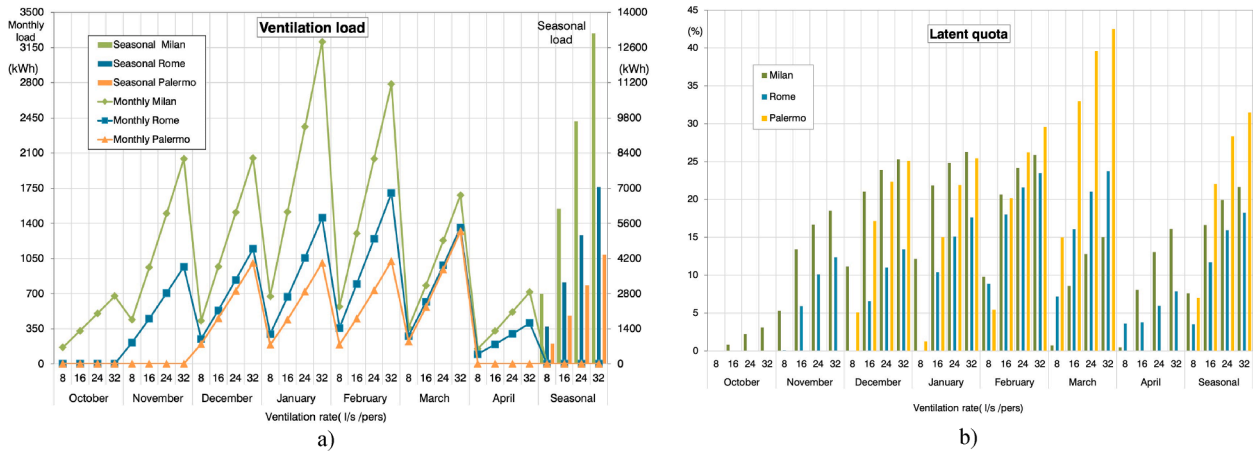


Fig. 4. Monthly and seasonal ventilation loads a) and relative percentage latent quotas b) for the four air flow rates in the three localities.

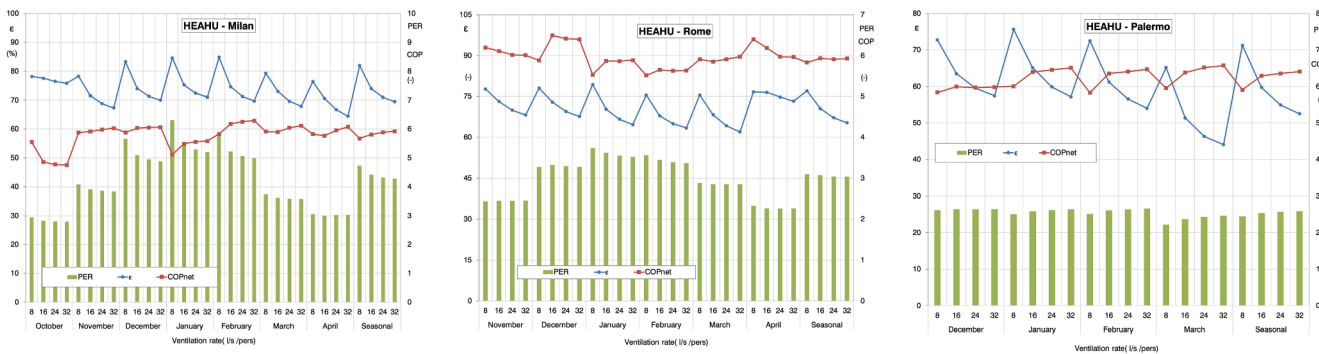


Fig. 5. Monthly and seasonal average percentage quotas  $\epsilon$ ,  $COP_{net}$  and PER with HEAHU.

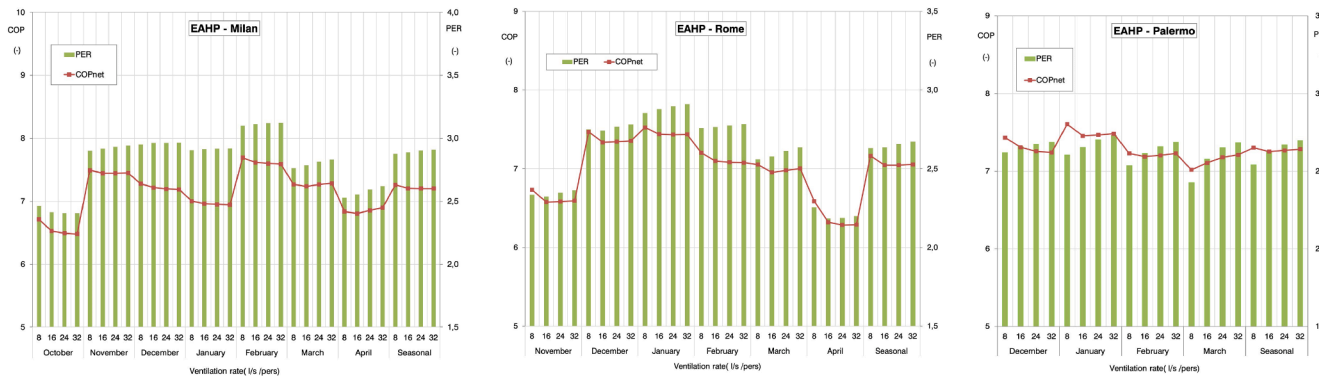


Fig. 6. Monthly and seasonal average  $COP_{net}$  and PER with EAHP.

trend of the average  $COP_{net}$  is influenced by the part load working in different modes in the various months and localities. The presence of a constant electric absorption of the fans in front of an extreme variability of the actual capacity supplied by the heat pump clearly affects average PERs which present a different trend as a function of the ventilation rate with respect to the corresponding trend of average  $COP_{net}$ .

Fig. 7 reports monthly and seasonal average percentage load quotas  $\epsilon$  and PERs with the OHR system. As inlet/outlet conditions are practically identical, the trends of the quotas  $\epsilon$  are the same as HEAHU. But in this case the remaining part of the ventilation load must be supplied by the condensing boiler. It involves a substantial decreasing of PER with a trend following the reduction of recuperator heat recovery.

The seasonal simulations highlighted that frost control intervenes only in Milan climatic condition. In the case of HEAHU (set point + 3 °C)

the total intervention hours are 59 and 19 with only recuperator system (set point + 1 °C).

However, in these hours, the fresh air supply quota deviated through the bypass damper is usually modest. To investigate the effects of frost control on energy performance, scenarios with or without (set point -10 °C) frost control intervention were compared. The penalization of seasonal PER is always not greater than 3.9% for HEAHU and 1.6% for the OHR system. Of course in Nordic climates the result can be quite different.

Fig. 8 presents a comparison of the seasonal performances of the three recovery systems. The net superiority of HEAHU PERs in Milan is quickly decreasing owing to the strong reduction of recuperator performance in milder climates in front of a significant fan electric absorption constant for each ventilation rate. For this reason, EAHP PERs



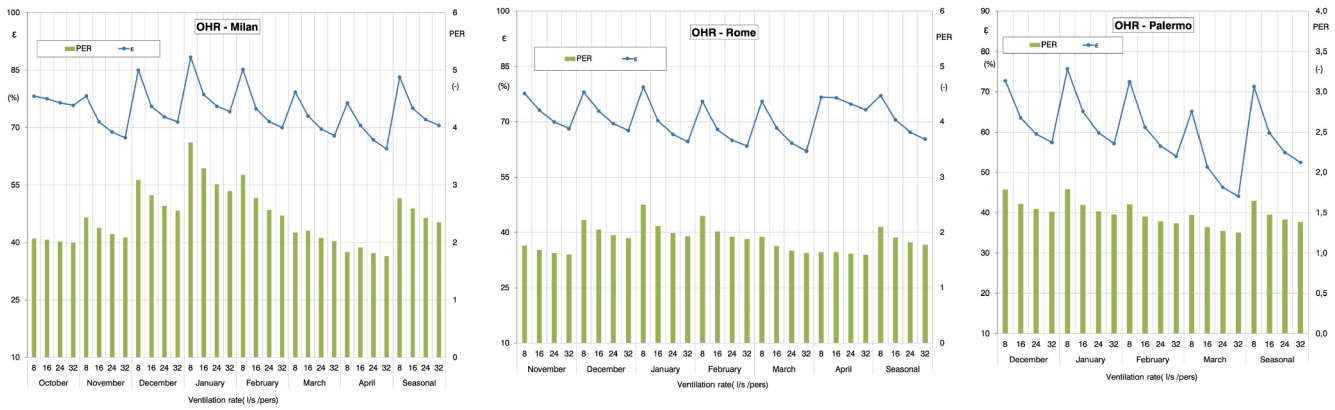


Fig. 7. Monthly and seasonal average percentage load quotas  $\epsilon$  and PERs with the OHR system.

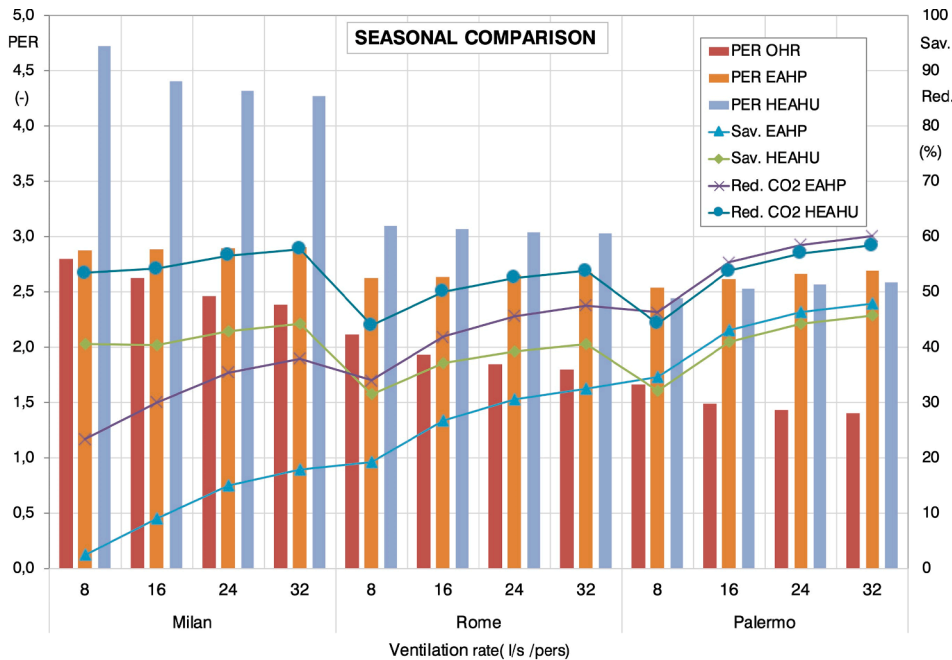


Fig 8. Seasonal PERs with the three recovery systems, energy savings and CO<sub>2</sub> emission reductions with HEAHU and EAHP referred to the corresponding primary consumptions and equivalent CO<sub>2</sub> emissions with the OHR system.

become slightly better than HEAHU PERs in Palermo. Even with the same climate, the OHR PERs decrease with the growth of air flow rate. This is due to the rise of the percentage latent quota of the total load as already observed in fig-4b. In fact consequently, the seasonal load, not covered by recovery and therefore provided by the boiler, is also increasing. To better clarify this fact, it is useful to consider a specific load here defined as the ratio between the load and the flow rate per person, For example, in Milan the specific total seasonal load goes from 348.8 to 411.2 kWh/(l/s/pers) when the flow rate changes from 8 l/s/pers to 32 l/s/pers. Of course, instead, the specific thermal recovery, 290 kWh/(l/s/pers), and the specific electrical consumption of the fans, 21.9 kWh/(l/s/pers), remain constant. Under these conditions the specific quota of heat to be supplied by the boiler increases from 58.8 to 121.1 kWh/(l/s/pers) reducing the seasonal PER. This reduction does not occur with EAHP and therefore it is smaller with HEAHU. In fact, in both cases the heat pump provides heat with PERs much higher than that one of the boiler which is 0.98 i.e. equal to its seasonal average thermal efficiency here assumed.

As the OHR system always presents the worst performance, it was used as a reference system to calculate the advantages permitted by the

other two alternative systems. In this way, the percentage saving of primary energy with HEAHU is variable between 31% and 46%. In the case of EAHP there is a wide oscillation of this saving from only 2.5% in Milan to 48% in Palermo. These calculated savings can be further improved remembering that the comparison does not consider pumping electric need to supply heat coil by hot water in the case of the OHR system. This consumption item could become significant in some real contexts. This outcome confirms the influence of the drastic performance reduction of the OHR system in Rome and Palermo. Regarding the effect of the ventilation rate increase in each city, Fig. 8 shows an improvement of this analysed saving for both the devices. Official data in Italy [81] were assumed to calculate the CO<sub>2</sub> emission. In particular for electric energy, a value of 0.308 Kg CO<sub>2</sub> per electric kWh which considers the mix of electric generating technologies used including renewable sources like hydro and photovoltaic plants. For the natural gas boiler an emission coefficient of 0.201 Kg CO<sub>2</sub> per kWh of primary energy consumption was used. Consequently, the seasonal reduction about CO<sub>2</sub> emission of HEAHU and EAHP were calculated compared to the emissions of the OHR system. This reduction is fluctuating in the range between 44% and 58% with HEAHU and between 23% and 60%

with EAHP. Noteworthy is the remarkable environmental benefit by EAHP vs the OHR system even when the superiority of the PER is modest. Of course the reason is the different CO<sub>2</sub> emission rate for natural gas and electric energy.

The use of OHR systems is well widespread in HVAC systems and relative commercial costs are available without problems for an extended variety of types and sizes. Unlike, the autonomous ventilation units implementing the HEAHU or EAHP solutions here studied have characteristics and sizes actually not existing in the market. This is particularly true for the EAHP solution which includes two condensers with an intermediate humidifier as a consequence of the requirement of a precise humidity control to contrast viral diffusion. A cost estimation of devices not existing on the market is considered unreliable in this phase and therefore it is postponed to a second stage of this study. For this reason a cost-benefit analysis is not provided in this discussion of the results.

#### 4. Conclusion

This work must be seen in the context of the current efforts by designers and companies to introduce new solutions and products in HVAC systems to better meet the pandemic emergency. On the basis of the assessment of their energy performances, the aim of this study is to individuate more suitable VHR systems to overcome possible energy and environmental barriers owing to the new ventilation exigencies required by the viral contrast. In this phase, the intent is to contribute to address the interest of manufacturers and designers towards the solutions here proposed. Successively, the indispensable financial comparison will be possible by using trusted costs provided by manufactures engaged to transform into commercial products these technical proposals.

The investigation has highlighted a behavioral sensitivity of the analyzed recovery systems to different amount of indoor latent gains and ventilation air flow rates. But first of all fundamental resulted the effect of the climatic condition which deeply affects the performances of the heat recuperator in milder climates. As consequence, the net superiority of HEAHU in Milan, thanks to the combined effects of heat pump and recuperator, is gradually reduced in Rome and Palermo. Here the benefit of the heat pump becomes predominant as consequence of the opportunity to take full advantage in the use of return air as a cold source at the evaporator. In Palermo the greater fan electric consumption due to the presence of the recuperator penalizes HEAHU versus EAHP. Naturally, in the event of a modest difference between the performances of two alternative systems, it will be the cost-benefit analysis to indicate the most convenient solution. This fact could happen with EAHP in Milan, where the quick reduction of the advantage with respect to the OHR system can suggest the use of the second device in case of lower initial cost. However, the same trend indicates the very likely superiority of the performance of the second device in Northern Europe climate even if not simulated in this study. In the end, the best solution is HEAHU in a colder climate and a recovery system based only on a heat pump with milder weather. The simulations highlight the possibility of great improvement in the installation of a heat pump in coupling or as an alternative to the more traditional OHR system. This statement is confirmed in the wide analyzed range of ventilation flow rates. In fact their possible extraordinary increment required by the viral contrast need strengthens the benefit. In comparison with OHR system consumption, by HEAHU primary energy saving can reach 46% in Milan and by EAHP 48% in Palermo. In conclusion, heat pump technology can give a fundamental contribution to reduce ventilation energy requirement. This possibility is particularly appreciable in presence of strong ventilation increments caused by the necessity to deal with a viral emergency like COVID-19. The reduction of CO<sub>2</sub> emission obtained by the heat pump is another important advantage in the context of the actions aimed at the reduction of greenhouse gas emissions.

#### Declaration of Competing Interest

The authors declare that they have no known competing financial interests or personal relationships that could have appeared to influence the work reported in this paper.

#### References

- [1] World Health Organization WHO (2020), Transmission of SARS-CoV-2: implications for infection prevention precautions, (2020).
- [2] J.W. Tang, Y. Li, I. Eames, P.K.S. Chan, G.L. Ridgway, Factors involved in the aerosol transmission of infection and control of ventilation in healthcare premises, *J. Hosp. Infect.* (2006), <https://doi.org/10.1016/j.jhin.2006.05.022>.
- [3] M. Nicas, W.W. Nazaroff, A. Hubbard, Toward understanding the risk of secondary airborne infection: Emission of respirable pathogens, *J. Occup. Environ. Hyg.* (2005), <https://doi.org/10.1080/15459620590918466>.
- [4] J. Wei, Y. Li, Airborne spread of infectious agents in the indoor environment, *Am. J. Infect. Control.* (2016), <https://doi.org/10.1016/j.ajic.2016.06.003>.
- [5] C.Y.H. Chao, M.P. Wan, L. Morawska, G.R. Johnson, Z.D. Ristovski, M. Hargreaves, K. Mengersen, S. Corbett, Y. Li, X. Xie, D. Katoshevski, Characterization of expiration air jets and droplet size distributions immediately at the mouth opening, *J. Aerosol Sci.* (2009), <https://doi.org/10.1016/j.jaerosci.2008.10.003>.
- [6] R.S. Papineni, F.S. Rosenthal, The size distribution of droplets in the exhaled breath of healthy human subjects, *J. Aerosol Med. Depos. Clear. Eff. Lung.* (1997), <https://doi.org/10.1089/jam.1997.10.105>.
- [7] D.A. Edwards, J.C. Man, P. Brand, J.P. Katstra, K. Sommerer, H.A. Stone, E. Warded, G. Scheuch, Inhaling to mitigate exhaled bioaerosols, *Proc. Natl. Acad. Sci. U. S. A.* (2004), <https://doi.org/10.1073/pnas.0408159101>.
- [8] M. Fang, A.P.S. Lau, C.K. Chan, C.T. Hung, T.W. Lee, Aerodynamic properties of biohazardous aerosols in hospitals, *Hong Kong. Med. J.* (2008).
- [9] P. Fabian, J.J. McDevitt, W.H. DeHaan, R.O.P. Fung, B.J. Cowling, K.H. Chan, G. M. Leung, D.K. Milton, Influenza virus in human exhaled breath: An observational study, *PLoS One.* (2008), <https://doi.org/10.1371/journal.pone.0002691>.
- [10] L. Morawska, G.R. Johnson, Z.D. Ristovski, M. Hargreaves, K. Mengersen, S. Corbett, C.Y.H. Chao, Y. Li, D. Katoshevski, Size distribution and sites of origin of droplets expelled from the human respiratory tract during expiratory activities, *J. Aerosol Sci.* 40 (2009) 256–269, <https://doi.org/10.1016/j.jaerosci.2008.11.002>.
- [11] A.C. Almstrand, B. Bake, E. Ljungström, P. Larsson, A. Bredberg, E. Mirgorodskaya, A.C. Olin, Effect of airway opening on production of exhaled particles, *J. Appl. Physiol.* (2010), <https://doi.org/10.1152/jappphysiol.00873.2009>.
- [12] World Health Organization(WHO), Infection prevention and control of epidemic and pandemic-prone acute respiratory infections in health care, WHO Guidel. (2014).
- [13] H. Qian, T. Miao, L. LIU, X. Zheng, D. Luo, Y. Li, Indoor transmission of SARS-CoV-2, *Indoor Air.* (2020).
- [14] L. Morawska, J.W. Tang, W. Bahnfleth, P.M. Bluyssen, A. Boerstra, G. Buonanno, J. Cao, S. Dancer, A. Floto, F. Franchimon, C. Haworth, J. Hogeling, C. Isaxon, J.L. Jimenez, J. Kurnitski, Y. Li, M. Loomans, G. Marks, L.C. Marr, L. Mazzarella, A.K. Melikov, S. Miller, D.K. Milton, W. Nazaroff, P. V. Nielsen, C. Noakes, J. Peccia, X. Querol, C. Sekhar, O. Seppänen, S. ichi Tanabe, R. Tellier, K.W. Tham, P. Wargocki, A. Wierzbicka, M. Yao, How can airborne transmission of COVID-19 indoors be minimised?, *Environ. Int.* (2020). Doi: 10.1016/j.envint.2020.105832.
- [15] R. Tellier, Review of aerosol transmission of influenza A virus, *Emerg. Infect. Dis.* (2006), <https://doi.org/10.3201/eid1211.060426>.
- [16] C.G. Loosli, H.M. Lemon, O.H. Robertson, E. Appel, Experimental Air-Borne Influenza Infection. I. Influence of Humidity on Survival of Virus in Air, *Proc. Soc. Exp. Biol. Med.* (1943), <https://doi.org/10.3181/00379727-53-14251P>.
- [17] M.Y.Y. Lai, P.K.C. Cheng, W.W.L. Lim, Survival of severe acute respiratory syndrome coronavirus, *Clin. Infect. Dis.* (2005), <https://doi.org/10.1086/433186>.
- [18] J. Gralton, E. Tovey, M.L. McLaws, W.D. Rawlinson, The role of particle size in aerosolized pathogen transmission: A review, *J. Infect.* (2011), <https://doi.org/10.1016/j.jinf.2010.11.010>.
- [19] R.J. Thomas, Particle size and pathogenicity in the respiratory tract, *Virulence.* (2013), <https://doi.org/10.4161/viru.27172>.
- [20] P.G. Koullapis, S.C. Kassinos, M.P. Bivolarova, A.K. Melikov, Particle deposition in a realistic geometry of the human conducting airways: Effects of inlet velocity profile, inhalation flowrate and electrostatic charge, *J. Biomech.* (2016), <https://doi.org/10.1016/j.jbiomech.2015.11.029>.
- [21] S. Tang, Y. Mao, R.M. Jones, Q. Tan, J.S. Ji, N. Li, J. Shen, Y. Lv, L. Pan, P. Ding, X. Wang, Y. Wang, C.R. MacIntyre, X. Shi, Aerosol transmission of SARS-CoV-2? Evidence, prevention and control, *Environ. Int.* (2020), <https://doi.org/10.1016/j.envint.2020.106039>.
- [22] Q.J. Leclerc, N.M. Fuller, L.E. Knight, S. Funk, G.M. Knight, What settings have been linked to SARS-CoV-2 transmission clusters? Wellcome Open Res. (2020) <https://doi.org/10.12688/wellcomeopenres.15889.2>.
- [23] Y. Li, G.M. Leung, J.W. Tang, X. Yang, C.Y.H. Chao, J.Z. Lin, J.W. Lu, P.V. Nielsen, J. Niu, H. Qian, A.C. Sleight, H.J.J. Su, J. Sundell, T.W. Wong, P.L. Yuen, Role of ventilation in airborne transmission of infectious agents in the built environment - A multidisciplinary systematic review, *Indoor Air.* (2007), <https://doi.org/10.1111/j.1600-0668.2006.00445.x>.
- [24] S. Xiao, Y. Li, M. Sung, J. Wei, Z. Yang, A study of the probable transmission routes of MERS-CoV during the first hospital outbreak in the Republic of Korea, *Indoor Air.* (2018), <https://doi.org/10.1111/ina.12430>.

- [25] G. Brankston, L. Gitterman, Z. Hirji, C. Lemieux, M. Gardam, Transmission of influenza A in human beings, *Lancet Infect. Dis.* (2007), [https://doi.org/10.1016/S1473-3099\(07\)70029-4](https://doi.org/10.1016/S1473-3099(07)70029-4).
- [26] B. Lopman, P. Gastanaduy, G.W. Park, A.J. Hall, U.D. Parashar, J. Vinjé, Environmental transmission of norovirus gastroenteritis, *Curr. Opin. Virol.* (2012), <https://doi.org/10.1016/j.coviro.2011.11.005>.
- [27] Z.T. Ai, A.K. Melikov, Airborne spread of expiratory droplet nuclei between the occupants of indoor environments: A review, *Indoor Air.* (2018), <https://doi.org/10.1111/ina.12465>.
- [28] E.J. Stewart, L.J. Schoen, K. Mead, C. Sekhar, R.N. Olmsted, W. Vernon, J. Pantelic, ASHRAE Position Document on Infectious Aerosols, *Ashrae.* (2020).
- [29] REHVA, How to operate and use building services in order to prevent the spread of the coronavirus disease (COVID-19) in workplaces, *Rehva.* (2020).
- [30] E.C. Riley, G. Murphy, R.L. Riley, Airborne spread of measles in a suburban elementary school, *Am. J. Epidemiol.* (1978), <https://doi.org/10.1093/oxfordjournals.aje.a112560>.
- [31] L. Gammitoni, M.C. Nucci, Using a Mathematical Model to Evaluate the Efficacy of TB Control Measures, *Emerg. Infect. Dis.* (1997), <https://doi.org/10.3201/eid0303.970310>.
- [32] G. Buonanno, L. Morawska, L. Stabile, Quantitative assessment of the risk of airborne transmission of SARS-CoV-2 infection: Prospective and retrospective applications, *Environ. Int.* (2020), <https://doi.org/10.1016/j.envint.2020.106112>.
- [33] K. Azuma, U. Yanagi, N. Kagi, H. Kim, M. Ogata, M. Hayashi, Environmental factors involved in SARS-CoV-2 transmission: effect and role of indoor environmental quality in the strategy for COVID-19 infection control, *Environ. Health Prev. Med.* (2020), <https://doi.org/10.1186/s12199-020-00904-2>.
- [34] L. Schibuola, M. Scarpa, C. Tambani, Natural Ventilation Level Assessment in a School Building by CO2 Concentration Measures, *Energy Procedia* (2016) 257–264, <https://doi.org/10.1016/j.egypro.2016.11.033>.
- [35] L. Schibuola, C. Tambani, Indoor environmental quality classification of school environments by monitoring PM and CO2 concentration levels, *Atmos. Pollut. Res.* (2019), <https://doi.org/10.1016/j.apr.2019.11.006>.
- [36] M. Santamouris, A. Synnefa, M. Assimakopoulos, I. Livada, K. Pavlou, M. Papaglastra, N. Gaitani, D. Kolokotsa, V. Assimakopoulos, Experimental investigation of the air flow and indoor carbon dioxide concentration in classrooms with intermittent natural ventilation, *Energy Build.* (2008), <https://doi.org/10.1016/j.enbuild.2008.04.002>.
- [37] REHVA, COVID-19 guidance document, (2020).
- [38] T. Circle, N.E. Atlanta, S. Fisher, T.M. Rainey, W.P. Bahnfleth, S. Campbell, A. K. Persily, G.M. Dobbis, D.L. Herron, D.S. Marciniak, ASHRAE Position Document on Infectious Aerosols, *Ashrae.* (2020).
- [39] Z. Yang, A. Ghahramani, B. Becerik-Gerber, Building occupancy diversity and HVAC (heating, ventilation, and air conditioning) system energy efficiency, *Energy.* 109 (2016) 641–649, <https://doi.org/10.1016/j.energy.2016.04.099>.
- [40] L. Schibuola, M. Scarpa, C. Tambani, Performance optimization of a demand controlled ventilation system by long term monitoring, *Energy Build.* 169 (2018), <https://doi.org/10.1016/j.enbuild.2018.03.059>.
- [41] S. Rotger-Grifol, R.H. Jacobsen, D. Nguyen, G. Sørensen, Demand response potential of ventilation systems in residential buildings, *Energy Build.* (2016), <https://doi.org/10.1016/j.enbuild.2016.03.061>.
- [42] L. Schibuola, M. Scarpa, C. Tambani, CO2 based ventilation control in energy retrofit: An experimental assessment, *Energy.* 143 (2018), <https://doi.org/10.1016/j.energy.2017.11.050>.
- [43] K. Ratajczak, E. Szczechowiak, Energy consumption decreasing strategy for indoor swimming pools – Decentralized Ventilation system with a heat pump, *Energy Build.* (2020), <https://doi.org/10.1016/j.enbuild.2019.109574>.
- [44] R.M. Lazzarin, G.A. Longo, Comparison of heat recovery systems in public indoor swimming pools, *Appl. Therm. Eng.* (1996), [https://doi.org/10.1016/1359-4311\(95\)00059-3](https://doi.org/10.1016/1359-4311(95)00059-3).
- [45] O. Ribé, R. Ruiz, M. Quera, J. Cadafalch, Analysis of the sensible and total ventilation energy recovery potential in different climate conditions. Application to the Spanish case, *Appl. Therm. Eng.* (2019), <https://doi.org/10.1016/j.applthermaleng.2018.12.076>.
- [46] L. Schibuola, High-efficiency recovery for air-conditioning applications in a mild climate: A case study, *Appl. Therm. Eng.* (1997), [https://doi.org/10.1016/s1359-4311\(96\)00051-8](https://doi.org/10.1016/s1359-4311(96)00051-8).
- [47] H. Han, M.-K. Kim, An Experimental Study on Air Leakage and Heat Transfer Characteristics of a Rotary-type Heat Recovery Ventilator, *Int. J. Air-Conditioning Refrig.* 13 (2005) 83–88.
- [48] G.V. Fracastoro, M. Serraino, Energy analyses of buildings equipped with exhaust air heat pumps (EAHP), *Energy Build.* (2010), <https://doi.org/10.1016/j.enbuild.2010.02.021>.
- [49] M. Thalfeldt, J. Kurnitski, E. Latšov, Exhaust air heat pump connection schemes and balanced heat recovery ventilation effect on district heat energy use and return temperature, *Appl. Therm. Eng.* (2018), <https://doi.org/10.1016/j.applthermaleng.2017.09.033>.
- [50] Z.Y. Zhang, C.L. Zhang, M.C. Ge, Y. Yu, A frost-free dedicated outdoor air system with exhaust air heat recovery, *Appl. Therm. Eng.* (2018), <https://doi.org/10.1016/j.applthermaleng.2017.09.091>.
- [51] EN 16798–1, Indoor environmental input parameters for design and assessment of energy performance of buildings- addressing indoor air quality, thermal environment, lighting and acoustics. (2019).
- [52] EN 16798–3, Ventilation for buildings – Part 3: For non-residential buildings – Performance requirements for ventilation and room conditioning systems (Modules M5–1, M5–4). (2017).
- [53] U.S. Department of Energy, EnergyPlus. (2019). <https://energyplus.net>.
- [54] J. Jokisalo, J. Kurnitski, M. Vuolle, A. Torkki, Performance of Balanced Ventilation with Heat Recovery in Residential Buildings in a Cold Climate, *Int. J. Vent.* (2003), <https://doi.org/10.1080/14733315.2003.11683667>.
- [55] M.K. Kim, L. Baldini, Energy analysis of a decentralized ventilation system compared with centralized ventilation systems in European climates: Based on review of analyses, *Energy Build.* (2016), <https://doi.org/10.1016/j.enbuild.2015.11.044>.
- [56] U. Aermec, Heat recovery units with cooling circuit: selection, use, installation and maintenance manual, technical bulletin 0313 (2020) 6180767\_07.
- [57] S. Taylor, M. Tasi, Low indoor-air humidity in an assisted living facility is correlated with increased patient illness and cognitive decline, *Indoor Air* (2018).
- [58] E. Kudo, E. Song, L.J. Yockey, T. Rakib, P.W. Wong, R.J. Homer, A. Iwasaki, Low ambient humidity impairs barrier function and innate resistance against influenza infection, *Proc. Natl. Acad. Sci. U. S. A.* (2019), <https://doi.org/10.1073/pnas.1902840116>.
- [59] W. Stone, O. Kroukamp, D.R. Korber, J. McKelvie, G.M. Wolfaardt, Microbes at surface-air interfaces: The metabolic harnessing of relative humidity, surface hygroscopicity, and oligotrophy for resilience, *Front. Microbiol.* (2016), <https://doi.org/10.3389/fmicb.2016.01563>.
- [60] B. Nourozi, Q. Wang, A. Ploskić, Energy and defrosting contributions of preheating cold supply air in buildings with balanced ventilation, *Appl. Therm. Eng.* (2019), <https://doi.org/10.1016/j.applthermaleng.2018.09.118>.
- [61] R. Ahmed, J. Appelhoff, Frost-protection measures in energy recuperation with multiple counterflow heat exchangers, *Rehva.* (2013).
- [62] J. Kragh, J. Rose, T.R. Nielsen, S. Svendsen, New counter flow heat exchanger designed for ventilation systems in cold climates, *Energy Build.* (2007), <https://doi.org/10.1016/j.enbuild.2006.12.008>.
- [63] A. Ploskić, Q. Wang, Reducing the defrosting needs of air-handling units by using heat from wastewater in apartment buildings in cold climates, *Appl. Therm. Eng.* (2019), <https://doi.org/10.1016/j.applthermaleng.2019.04.057>.
- [64] AERMEC, Heat recovery units with cooling circuit: selection, use, installation and maintenance manual, technical bulletin 0313 (2020) 6180767\_07.
- [65] Clivet, ELFOFresh Large, Heat recovery with reversible heat pump, technical bulletin, BT05L001GB. (2013).
- [66] Rhoss, UTRN-A Platinum, Heat recovery series, Installation, use and maintenance manual, technical bulletin H58251 F 11.18. (2020).
- [67] NSAI, EN 308: Heat Exchangers - Test Procedures For Establishing Performance of Air to Air and Flue Gases Heat Recovery Devices. (1997).
- [68] S.A. Klein, TRNSYS 17: A Transient System Simulation Program, *Sol. Energy Lab. Univ. Wisconsin, Madison, USA.* 2010.
- [69] DOE, EnergyPlus | EnergyPlus, U.S. Dep. Energy's. (2017).
- [70] AHRI, Performance Rating of Air-to-Air Exchangers for Energy Recovery Ventilation Equipment, AHRI 1060, AHRI Stand. (2013).
- [71] ASHRAE, Psychrometric theory and practice. (1996).
- [72] ASHRAE, Handbook / Fundamentals, chapter 1 Psychrometrics. (2017).
- [73] EN 14511-3:2019 Air conditioners, liquid chilling packages and heat pumps for space heating and cooling and process chillers, with electrically driven compressors Part 3: Tests Methods. (2019).
- [74] CEN, EN 14825:2018 Air conditioners, liquid chilling packages and heat pumps, with electrically driven, compressors, for space heating and cooling - Testing and rating at part load conditions and calculation of seasonal performance, (2018) 139.
- [75] L. Schibuola, Heat pump seasonal performance evaluation: A proposal for a European standard, *Appl. Therm. Eng.* (2000), [https://doi.org/10.1016/S1359-4311\(99\)00041-1](https://doi.org/10.1016/S1359-4311(99)00041-1).
- [76] M. Dongellini, C. Naldi, G.L. Morini, Seasonal performance evaluation of electric air-to-water heat pump systems, *Appl. Therm. Eng.* (2015), <https://doi.org/10.1016/j.applthermaleng.2015.03.026>.
- [77] S. In, K. Cho, B. Lim, C. Lee, Partial load performance test of residential heat pump system with low-GWP refrigerants, *Appl. Therm. Eng.* (2015), <https://doi.org/10.1016/j.applthermaleng.2015.04.013>.
- [78] E. Bettanini, A. Gastaldello, L. Schibuola, Simplified models to simulate part load performances of air conditioning equipments, in: Eighth Int. IBPSA Conf. Eindhoven, Netherlands August 11-14. (2003).
- [79] DM 26 giugno 2015, Applicazione delle metodologie di calcolo delle prestazioni energetiche e definizione delle prescrizioni e dei requisiti minimi degli edifici. (2015).
- [80] UNI/TS 11300:2, Energy Performance of Buildings, Technical Specification, Italian standard 2014. (2014).
- [81] Ispra, Greenhouse gas emission factors in the national electricity sector and in the main European countries, report 303, (2019).